JAWS coordinates chondrogenesis and synovial joint positioning

Michael L. Sohaskey[1],*, Jane Yu[1], Michael A. Diaz[2], Anna H. Plaas[2] and Richard M. Harland[1],*

Properly positioned synovial joints are crucial to coordinated skeletal movement. Despite their importance for skeletal development and function, the molecular mechanisms that underlie joint positioning are not well understood. We show that mice carrying an insertional mutation in a previously uncharacterized gene, which we have named *Jaws* (joints abnormal with splitting), die perinatally with striking skeletal defects, including ectopic interphalangeal joints. These ectopic joints develop along the longitudinal axis and persist at birth, suggesting that JAWS is uniquely required for the orientation and consequent positioning of interphalangeal joints within the endochondral skeleton. *Jaws* mutant mice also exhibit severe chondrodysplasia characterized by delayed and disorganized maturation of growth plate chondrocytes, together with impaired chondroitin sulfation and abnormal metabolism of the chondroitin sulfate proteoglycan aggrecan. Our findings identify JAWS as a key regulator of chondrogenesis and synovial joint positioning required for the restriction of joint formation to discrete stereotyped locations in the embryonic skeleton.

KEY WORDS: Chondrogenesis, Synovial joints, Interzone, Gdf5, Chondroitin sulfate, Extracellular matrix, Mouse embryo

INTRODUCTION

Synovial joints segment the developing cartilage template into individual skeletal elements while providing flexibility and structural stability between these elements. Histologically, the earliest sign of synovial joint formation is the appearance of the interzone (Mitrovic, 1977), which occurs at approximately embryonic day (E) 12.5-13.5 in mouse digits. Several signaling pathways are implicated in the molecular specification of the joint interzone, including those downstream of the secreted proteins growth differentiation factor 5 (Gdf5) and Wnt9a (Hartmann and Tabin, 2001; Pacifici et al., 2005; Khan et al., 2007). By contrast, the molecular mechanisms that control spatial positioning of the joint interzone are not well understood. Here we identify a previously uncharacterized protein, which we have named JAWS (joints abnormal with splitting), as a novel and essential coordinator of cartilage formation and synovial joint positioning.

MATERIALS AND METHODS

Animals

The KST245 mouse embryonic stem cell line, containing an insertion of the pGT1TMpfs gene trap vector in the *Jaws/Impad1* locus, was isolated and characterized as described (Mitchell et al., 2001). *Jaws* F1 heterozygotes were backcrossed to C57BL/6 mice for six generations before intercrossing. Genotyping was performed by X-gal staining of yolk sacs and/or tail biopsies, or by RT-PCR using primers flanking the insertion site (sequences available upon request).

Expression studies

Jaws transcripts were detected by northern blotting of Trizol-extracted total RNA, probed with a cDNA fragment spanning nucleotides 726-1158 of the *Jaws* mRNA (GenBank Accession Number BC145952). Alternatively, *Jaws* expression was assessed by quantitative RT-PCR using SYBR Green reagents (Applied Biosystems). For immunoblotting of E13.5 embryo lysates (60 μg), a polyclonal antiserum was raised against the peptide epitope N-CRESNVLHEKSKGKTREGADD-C corresponding to residues 83-102 of the JAWS protein.

Histology, in situ hybridization and immunohistochemistry

Alcian Blue and Alizarin Red staining of skeletal preparations and histological sections, X-gal staining of embryos, and in situ hybridization were performed as described (Nagy, 2003). To enhance contrast against the Hoechst counterstain, the radioactive ISH images were photographed in bright-field and then pseudo-colored red using the 'Colorize' option within the 'Hue/Saturation' command in Adobe Photoshop 7.0. Immunohistochemistry on paraffin sections was carried out after antigen retrieval, using Alexa Fluor-conjugated secondary antibodies and the following primary antibodies: mouse aggrecan 12/21/1-C-6 and link protein 9/30/8-A-4 (Developmental Studies Hybridoma Bank), mouse β-catenin (BD Biosciences), mouse chondroitin sulfate CS-56 (Sigma-Aldrich), rabbit collagen II (Abcam) and rat CD44S (Chemicon). Apoptotic cells were labeled using the In Situ Cell Death Detection kit (Roche).

Fluorophore-assisted carbohydrate electrophoresis (FACE)

The composition and amount of chondroitin sulfate and heparan sulfate were analyzed as described (Plaas et al., 2001; Gao et al., 2004). Values for total CS, HS and HA were normalized to wet tissue weight. FACE data were analyzed by a two-tailed Student's *t*-test, and values were considered statistically significant at $P<0.05$.

Protein extraction and aggrecan immunoblotting

Successive nondissociative extractions (0.15 M NaCl, then 0.15 M NaCl + 0.5% CHAPS) of E14.5 limb tissue were followed by one dissociative extraction (4 M guanidinium HCl + 0.5% CHAPS) to solubilize matrix-associated proteins. Loadings for SDS-PAGE were normalized to wet tissue weight, and immunoblots were processed with polyclonal CDAGWL antibodies directed against the N-terminal G1 domain of aggrecan. Blots were exposed to film simultaneously and developed identically.

RESULTS AND DISCUSSION

JAWS is required for the development of the endochondral skeleton

Jaws (also known as *Impad1* – Mouse Genome Informatics) was identified in an insertional mutagenesis screen for genes encoding secreted and transmembrane proteins essential for mammalian development (Mitchell et al., 2001). The *Jaws/Impad1* locus encodes a predicted protein of ~39 kDa with an N-terminal hydrophobic domain and a consensus inositol monophosphatase

[1]Division of Genetics, Genomics and Development, Department of Molecular and Cell Biology, Center for Integrative Genomics, University of California, Berkeley, CA 94720, USA. [2]Departments of Internal Medicine (Rheumatology) and Biochemistry, Rush University Medical Center, 1725 Harrison Street, Chicago, IL 60612, USA.

*Authors for correspondence (e-mail: sohaskey@berkeley.edu; harland@berkeley.edu)

catalytic motif. Insertion of the gene-trap vector into the third of four introns fuses the first 213 amino acids of the JAWS protein in-frame with a βgeo reporter, resulting in less than 0.2% expression of wild-type (WT) transcripts and negligible expression of the endogenous protein (see Fig. S1 in the supplementary material). Together with the observation that βgeo fusion proteins generated by this 'secretory trap' accumulate in cytoplasmic inclusion bodies (Skarnes et al., 1995; Mitchell et al., 2001), these data suggest that the *Jaws* insertion creates a null or strongly hypomorphic allele.

Jaws mRNA and protein expression is widespread during embryogenesis and early postnatal life (Fig. 1A; see Fig. S1 in the supplementary material). In the developing skeleton, X-gal staining demonstrated β-galactosidase activity throughout the cartilage growth plate and in primary ossification centers, with prominent staining in chondrogenic condensations, perichondrium and articular chondrocytes (Fig. 1A; data not shown).

Mice carrying one copy of the *Jaws* insertional mutation (*Jaws*^{+/–}) appeared phenotypically indistinguishable from wild-type littermates. By contrast, mice homozygous for the insertion (*Jaws*^{–/–}) died perinatally with cleft secondary palate (see Fig. S2 in the supplementary material). *Jaws*^{–/–} neonates exhibited severe dwarfism with stunted limbs, hypoplastic ribcages and rounder shortened craniofacies (Fig. 1B,C). The cranial vault and clavicles, which form without a cartilage intermediate, were largely unaffected (Fig. 1C; data not shown). These results reveal that the skeletal defects in *Jaws*^{–/–} embryos were restricted to elements formed through endochondral ossification. Defects in chondrogenesis were apparent by E12.5 in *Jaws*^{–/–} embryos (see Fig. S3 in the supplementary material), despite robust expression of the chondrogenic markers *Sox9*, *Sox5* and *Col2a1* (see Fig. S4 in the supplementary material) (Akiyama et al., 2002). This latter observation suggests that JAWS is dispensable for the formation of prechondrogenic condensations from limb bud mesenchyme.

In the embryonic growth plate, chondrocytes align in a pseudocolumnar arrangement along the longitudinal axis according to their differentiation status, which is reflected in the demarcation of four histologically and molecularly distinct chondrocytic zones: resting, proliferative, prehypertrophic and hypertrophic (Kronenberg, 2003). Histologically, *Jaws*^{–/–} chondrocytes lacked the pseudocolumnar organization of their wild-type counterparts (Fig. 1D). Mutant growth plates were hypocellular, with discontinuities in Alcian Blue staining revealing regions devoid of extracellular matrix (ECM). After E15.5, ectopic chondrocytes were regularly seen impinging on the primary ossification center in *Jaws*^{–/–} embryos (Fig. 1D, arrow).

JAWS deficiency delays chondrocyte maturation and disrupts long-range Ihh signaling in the growth plate

To analyze growth plate maturation in molecular detail, we examined markers of chondrocyte differentiation by in situ hybridization at E14.5 (Fig. 2A). Expression of the proliferating chondrocyte marker *Col2a1* was largely excluded from the central *Col10a1*-expressing hypertrophic zone in wild-type long bones, whereas in *Jaws*^{–/–} embryos *Col2a1* expression partially overlapped this *Col10a1* domain. During hypertrophic differentiation, maturing chondrocytes abruptly switch from *Col2a1* to *Col10a1* expression; thus, this overlap in the two domains suggests that many *Jaws*^{–/–} chondrocytes were in a delayed intermediate state of already expressing *Col10a1* without yet having downregulated *Col2a1* expression (St-Jacques et al., 1999). Similarly, wild-type expression of *Ihh* or *Pthr* appeared in symmetrical domains of prehypertrophic
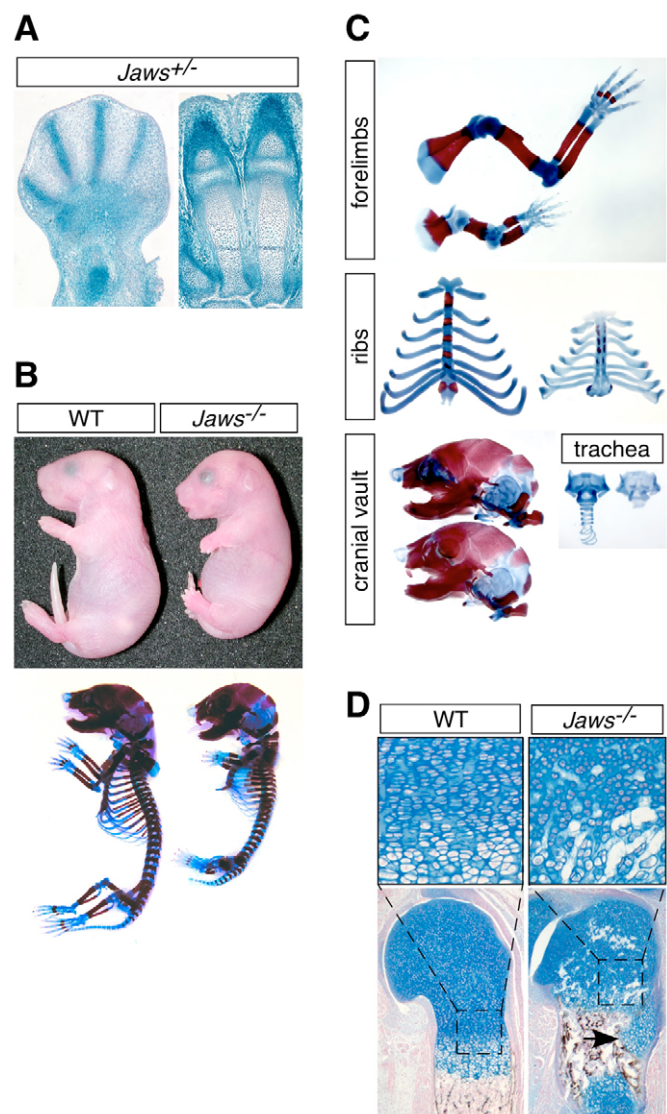

Fig. 1. Insertional mutagenesis of *Jaws* causes chondrodysplasia. (**A**) Widespread β-galactosidase staining from the gene trap reporter in *Jaws*^{+/–} E12.5 forelimb (left) and E15.5 digits (right). (**B**) Gross morphology (top) and cleared skeletal preparations (bottom) of wild-type (WT) and *Jaws*^{–/–} embryos (E18.5). (**C**) Skeletal preparations from wild-type (top or left) and *Jaws*^{–/–} (bottom or right) embryos, showing severe malformation of endochondral elements. (**D**) Alcian Blue/von Kossa staining of humerus sections (E17.5). The arrow indicates ectopic chondrocytes encroaching upon the primary ossification center. Higher-magnification views (top) show hypocellularity and ECM discontinuity in the *Jaws*^{–/–} growth plate.

chondrocytes flanking the central *Col10a1* domain (Kronenberg, 2003); however, one continuous domain of expression overlapping that of *Col10a1* was seen for each gene in *Jaws*^{–/–} embryos. Altered expression of two downstream targets of Ihh signaling, *Ptch1* and *Pthrp*, was also evident. *Ptch1* expression was unchanged in the perichondrium and proliferating chondrocytes proximal to the Ihh source in *Jaws*^{–/–} embryos; however, expression of *Ptch1* in resting and periarticular chondrocytes was markedly diminished, as was expression of *Pthrp* (Fig. 2A, arrows). This finding implies normal short-range, but disrupted long-range, Ihh signaling in the *Jaws*^{–/–} growth plate, probably resulting from compromised ECM integrity
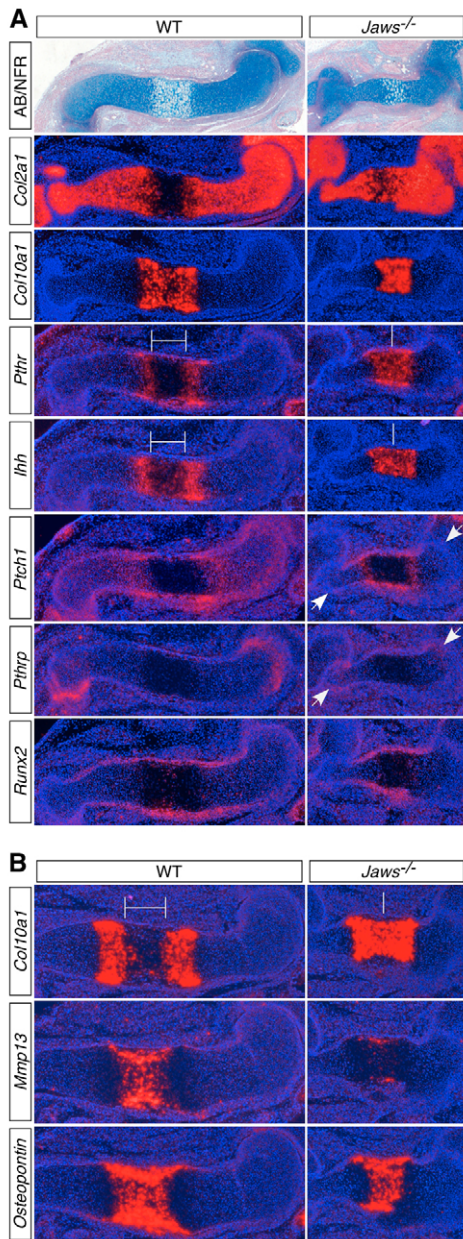
Fig. 2. *Jaws*⁻/⁻ **embryos exhibit delayed chondrocyte maturation.**
(**A**) Histological and radioactive in situ hybridization analysis of
chondrocyte maturation in the humerus (E14.5). Top panels show
sections stained with Alcian Blue and nuclear Fast Red (AB/NFR). White
brackets indicate the separation of wild-type prehypertrophic zones,
which remain continuous in the *Jaws*⁻/⁻ embryo (vertical lines). Arrows
indicate reduced *Ptch1* and *Pthrp* signals in periarticular chondrocytes.
(**B**) Radioactive in situ hybridization analysis showing delayed terminal
hypertrophic chondrocyte differentiation in the *Jaws*⁻/⁻ humerus
(E15.5), evidenced by decreased expression of *Mmp13* and
osteopontin. White brackets indicate the separation of wild-type
Col10a1-positive hypertrophic zones, which remain continuous in the
Jaws⁻/⁻ embryo (vertical line).

(see below). Collectively, these data indicate a delay in chondrocyte
maturation in *Jaws*⁻/⁻ embryos. Terminal hypertrophic chondrocyte
differentiation was also delayed in E15.5 *Jaws*⁻/⁻ cartilage, as
evidenced by a persistent central domain of *Col10a1* expression and
reduced expression of the terminal differentiation markers *Mmp13*

and osteopontin (*Spp1*) (Fig. 2B). Delayed chondrocyte maturation
was most conspicuous in the hindlimb, where the knee joint failed
to form and where the tibia retained a homogeneous population of
small, *Col2a1*-expressing chondrocytes at E18.5 (Fig. 3A; see Fig.
S5 in the supplementary material). Finally, expression of the
osteoprogenitor markers *Runx2* (Kronenberg, 2003) and *Tcf1* (Glass,
2nd et al., 2005) was similar in wild-type and *Jaws*⁻/⁻ long bones,
excluding the tibia (Fig. 2A; data not shown), suggesting that
subsequent osteogenesis, when it occurred, initiated normally.

Ectopic joints form in the digits of *Jaws*⁻/⁻ mice

The most striking defect in *Jaws*⁻/⁻ embryos was seen in the digits,
where skeletal preparations revealed longitudinally oriented cavities
that lacked Alcian Blue staining and were flanked by cartilage (Fig.
3A). These nonchondrogenic cavities, which were first apparent
when the wild-type interzone formed at ~E13.5, extended from the
presumptive metacarpophalangeal/metatarsophalangeal joint to the
distalmost phalanx in all digits, appearing discontinuous in
forelimbs while bisecting and spanning each hindlimb element. Two
main possibilities could explain the occurrence of these cavities:
either they result from aberrant cell death, or they represent ectopic
joints. To distinguish these possibilities, we first examined the early
joint marker *Gdf5* by whole-mount in situ hybridization and found
that *Gdf5* expression extended longitudinally throughout these
cavities (Fig. 3B; Fig. S6 in the supplementary material). Likewise,
expression of all joint markers examined, including *Gli3*, *Wnt9a*,
Sulf1, *Cutl1* (*Cux1*), *Stc1*, *Hip1* and activated β-catenin (Guo et al.,
2004; Hill et al., 2005; Pacifici et al., 2005; Mak et al., 2006; Zhao
et al., 2006; Khan et al., 2007) overlapped the *Gdf5* expression
domain (Fig. 3C and data not shown), suggesting that cells within
these cavities exhibited a joint-like fate. Histologically, these cells
resembled wild-type joint progenitors in having a flattened, more
mesenchymal appearance than surrounding chondrocytes (Fig. 3C;
data not shown). TUNEL analysis demonstrated similar numbers of
apoptotic cells in wild-type and *Jaws*⁻/⁻ joints at all stages examined
(E12.5-E17.5; see Fig. S7 in the supplementary material, and data
not shown), further excluding cell death as a disproportionate
contributor to the joint phenotype. Likewise, consistent cartilage
staining in the digits of E12.5 *Jaws*⁻/⁻ autopods prior to the
appearance of the joint interzone suggested that ectopic joints were
not a secondary consequence of diminished ECM formation (see
Fig. S3 in the supplementary material; data not shown). Moreover,
no changes in the expression of limb polarity markers were evident
earlier in E11.5 or E12.5 *Jaws*⁻/⁻ embryos (see Fig. S8 in the
supplementary material).

If the longitudinal cavities in *Jaws*⁻/⁻ digits represent joints, then
they should not only express joint markers but also exclude markers
of neighboring cell types. Indeed, expression of the chondrogenic
markers collagen 2, aggrecan and link protein was excluded from
prospective *Jaws*⁻/⁻ joints (Fig. 3D and data not shown) (Schwartz
and Domowicz, 2002). Similarly, expression of *Bmpr1b*, which is
normally restricted to articular surfaces flanking the wild-type joint
interzone at E14.5 (Baur et al., 2000; Yi et al., 2000), was seen in an
analogous pattern bordering the longitudinal domain of *Gdf5*
expression in *Jaws*⁻/⁻ digits (Fig. 3D). Thus, joint-like structures in
Jaws⁻/⁻ digits do not express chondrogenic markers but do maintain
their immediate proximity to *Bmpr1b*-expressing articular
chondrocytes. In addition, these joint-like structures did not express
markers of hypertrophic chondrocytes (*Col10a1*) or osteoblasts
(*Runx2*), while expressing wild-type levels of the tendon and
ligament marker *Scx* (Fig. 3E) (Schweitzer et al., 2001).
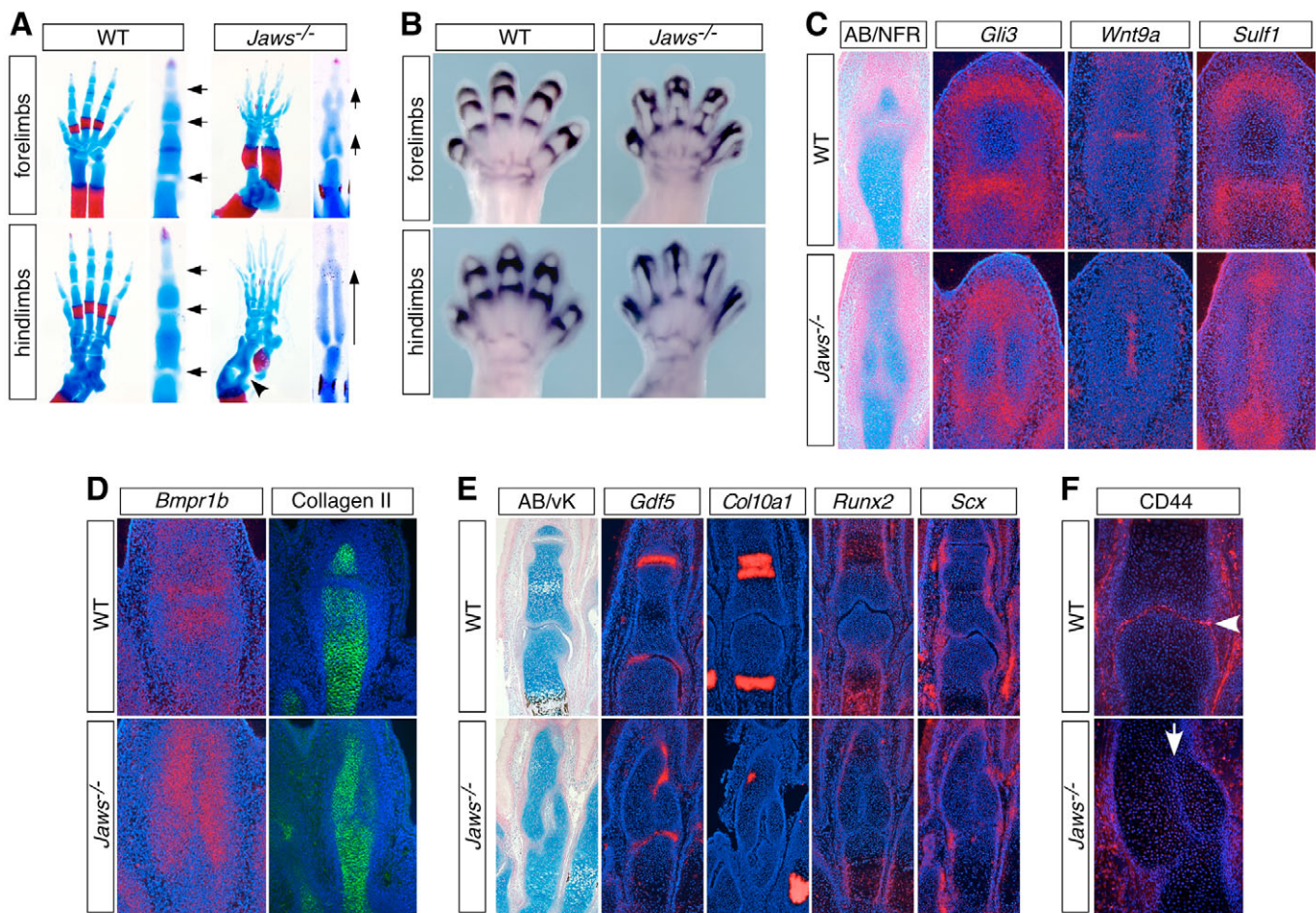Collectively, these molecular and histological data establish the

Fig. 3. *Jaws*⁻ᐟ⁻ digits develop ectopic joints. (A) Longitudinal cavities lacking Alcian Blue staining form in *Jaws*⁻ᐟ⁻ digits (E18.5). Higher-magnification views of digit 3 are shown to the right of each limb, with arrows indicating joint position and orientation. The arrowhead indicates failed knee joint formation proximal to a lack of tibial ossification in the *Jaws*⁻ᐟ⁻ hindlimb. **(B)** Whole-mount in situ hybridization for *Gdf5* expression (E14.5). **(C)** Histological and in situ hybridization analysis showing longitudinal expression of joint interzone markers in individual *Jaws*⁻ᐟ⁻ hindlimb digits (E14.5). **(D)** Exclusion of *Bmpr1b* RNA and collagen 2 protein expression from ectopic *Jaws*⁻ᐟ⁻ joints (E14.5). **(E)** Ectopic joints express *Gdf5* but not markers of hypertrophic chondrocytes (*Col10a1*), osteoblasts (*Runx2*), or tendons and ligaments (*Scx*) (E18.5 forelimb digits). AB/vK, Alcian Blue/von Kossa. **(F)** Defective cavitation of E18.5 ectopic joint (arrow), evidenced by the absence of CD44 immunostaining (arrowhead, wild-type staining).

longitudinal cavities in *Jaws*⁻ᐟ⁻ digits as ectopic joints. The persistence of ectopic joints in neonatal *Jaws*⁻ᐟ⁻ mice defines JAWS as a crucial novel regulator of synovial joint orientation and positioning. Because misorientation of the interzone necessarily causes an ectopic joint, we use the terms 'orientation' and 'positioning' interchangeably here.

Cavitation is the late-stage process culminating in formation of the synovial cavity. Cavitation in E18.5 wild-type forelimb digits was demonstrated by expression of the hyaluronan (HA) receptor CD44 on articular surfaces (Pitsillides, 1999). By contrast, CD44 immunostaining was largely absent from ectopic *Jaws*⁻ᐟ⁻ joints, despite its presence in more proximal joints (Fig. 3F; data not shown). This result indicates a requirement for JAWS in the timely progression to cavitation, leading to a functional synovial joint.

Impaired chondroitin sulfation and aberrant aggrecan metabolism in *Jaws*⁻ᐟ⁻ cartilage

From a mechanistic perspective, several features of the *Jaws*⁻ᐟ⁻ phenotype are consistent with defects in chondroitin sulfation pathways. In particular, misaligned chondrocytes, hypocellularity and ECM discontinuities characterize the growth plates of animals

lacking chondroitin-4-sulfotransferase 1 (*C4st1*; *Chst11* – Mouse Genome Informatics) or the chondroitin sulfate (CS)- and heparan sulfate (HS)-rich proteoglycan perlecan (Klüppel et al., 2005; Schwartz and Domowicz, 2002). Moreover, mutant mice lacking components of the CS synthesis or transport machinery are chondrodysplastic (Schwartz and Domowicz, 2002). For these reasons, we examined whether CS was spatially or quantitatively altered in *Jaws*⁻ᐟ⁻ embryos. Immunostaining for CS demonstrated highest levels in the perichondrium and articular zones of E14.5 limbs (Fig. 4A; data not shown), with intense uniform extracellular staining in wid-type digits. By contrast, a faint punctate pattern was observed in *Jaws*⁻ᐟ⁻ digits, much of which appeared to localize intracellularly (Fig. 4A, insets).

We then used fluorophore-assisted carbohydrate electrophoresis to analyze and quantify glycosaminoglycan content in E14.5 limbs. Consistent with our immunostaining data, significant decreases in the proportions of both chondroitin-4-sulfate (C4S) and chondroitin-6-sulfate (C6S) were evident in *Jaws*⁻ᐟ⁻ limbs, with concomitant increases in unsulfated chondroitin (C0S) (Fig. 4B). Importantly, no change in heparan sulfation was observed (Fig. 4C). Moreover, quantities of total CS (including C0S), HS and HA normalized to
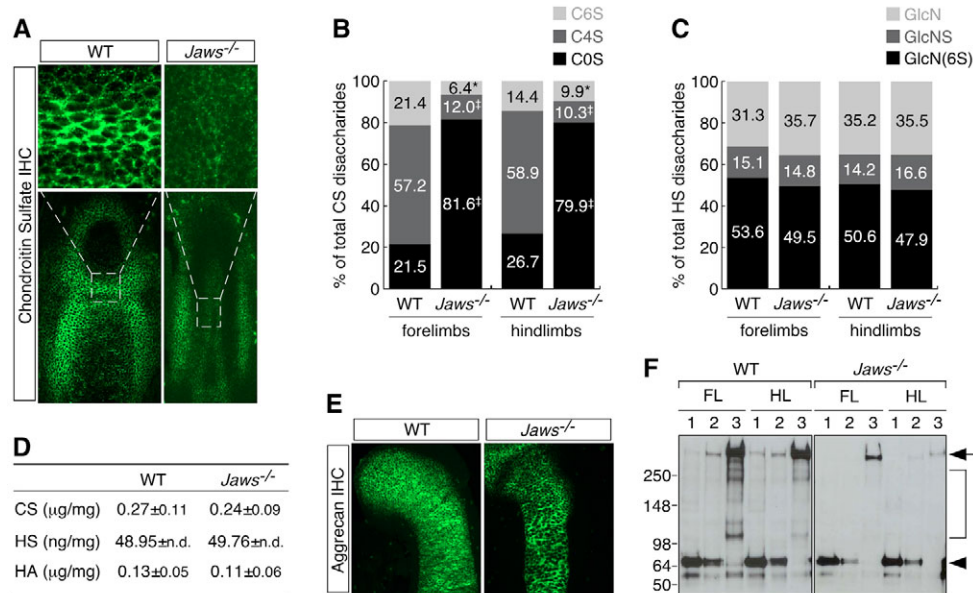
Fig. 4. Impaired chondroitin sulfation and altered aggrecan metabolism in *Jaws*$^{-/-}$ limbs. (**A**) CS immunostaining in hindlimb digits (E14.5). Higher-magnification views (top) reveal sparse irregular staining in the *Jaws*$^{-/-}$ joint. (**B,C**) Fluorophore-assisted carbohydrate electrophoresis analysis of chondroitin sulfate (CS, B) and heparan sulfate (HS, C) in E14.5 limbs. The relative proportions and percentages of disaccharides generated with the glycosaminoglycan-specific lysases are shown. For HS, no disaccharides containing 2-sulfated uronic acid (UA) or N,6-sulfated GlcN were detected. galNAc, N-acetylgalactosamine; C0S, ΔUA-galNAc; C4S, ΔUA-galNAc4S; C6S, ΔUA-galNAc6S; glcNAc, N-acetylglucosamine; GlcN, ΔUA-glcNAc; GlcNS, ΔUA-glcNS; GlcN(6S), ΔUA-glcNAc6S. *$P<0.025$; ‡$P<0.0001$, *Jaws*$^{-/-}$ versus wild type percentage ($n=5$ pairs per genotype). (**D**) Comparable amounts (mean and s.d.) of total glycosaminoglycans in wild type and *Jaws*$^{-/-}$ hindlimbs, normalized to wet tissue weight. Similar results were obtained for forelimbs. n.d., not determined; HA, hyaluronan. (**E**) Aggrecan immunostaining in the proximal end of the humerus (E14.5). (**F**) Anti-CDAGWL immunoblots of E14.5 limb protein extracts, showing less full-length aggrecan (arrow, ~350 kDa) and fewer aggrecan cleavage fragments (bracket) in *Jaws*$^{-/-}$ cartilage. Successive nondissociative extractions (lanes 1 and 2; arrowhead indicates a 65 kDa proteolytic fragment) were followed by one dissociative extraction (lane 3). HL, hindlimbs; FL, forelimbs.

wet tissue weight were comparable in wild-type and *Jaws*$^{-/-}$ limbs (Fig. 4D). The expression of *C4st1*, *Slc26a2* and *Papss2* – key regulators of CS biosynthesis and/or transport – was also unchanged, implying that JAWS does not influence CS levels through transcriptional regulation of these genes (see Fig. S9 in the supplementary material). As described above, this specific diminution of chondroitin sulfation is consistent with the *Jaws*$^{-/-}$ growth plate defects and suggests a molecular mechanism by which JAWS coordinates chondrogenesis and joint positioning. As extracellular HS is important for shaping the Ihh morphogen gradient (Koziel et al., 2004), these data also argue that the disruption of long-range Ihh signaling in the *Jaws*$^{-/-}$ growth plate (Fig. 2A) does not result from a change in HS levels but from a generalized loss of ECM integrity.

Decreased chondroitin sulfation may affect chondrogenesis in part by disrupting the normal metabolism of CS-containing proteoglycans such as aggrecan. Aggrecan is the predominant CS proteoglycan of the cartilage matrix and is crucial to normal chondrogenesis and ECM integrity (Schwartz and Domowicz, 2002). The CS chains of aggrecan are essential for its efficient secretion and for binding and proteolytic cleavage by the aggrecanase Adamts4 (Kiani et al., 2001; Tortorella et al., 2000). Therefore, we assessed whether *Jaws*$^{-/-}$ embryos show impaired expression and/or turnover of aggrecan. Aggrecan immunostaining revealed mottled, variable expression throughout E14.5 *Jaws*$^{-/-}$ cartilage, in contrast to the robust consistent wild-type staining pattern (Fig. 4E and data not shown). Notably, mRNA and protein levels of two other abundant cartilage ECM proteins, collagen 2 and link protein, were unchanged, suggesting that abnormal aggrecan expression was not a secondary consequence of delayed

chondrocyte maturation (see Fig. S10 in the supplementary material; data not shown). To confirm and extend this aggrecan result, an antibody (anti-CDAGWL) that recognizes intact aggrecan and several well-characterized cleavage products was used to analyze limb protein extracts (Arner, 2002). Under dissociative conditions, markedly reduced amounts of both full-length aggrecan (Fig. 4F, arrow) and C-terminally cleaved aggrecan fragments (Fig. 4F, bracket) were extracted from *Jaws*$^{-/-}$ relative to wild-type limbs. This reduction was greater in hindlimbs, where more severe chondrogenic and joint defects were noted (Fig. 3A; Fig. S5 in the supplementary material). As an internal control, successive nondissociative extractions yielded similar levels of a 65 kDa aggrecan fragment that is likely to result from transient expression and rapid cleavage in extracartilaginous tissue (Fig. 4F, arrowhead) (Arner, 2002). Collectively, these data suggest that impaired CS sulfation and abnormal aggrecan metabolism contribute to the chondrodysplasia and aberrant joint positioning in *Jaws*$^{-/-}$ embryos.

Although the precise mechanism by which JAWS influences CS sulfation and ECM integrity is unclear, CS sulfation has been reported to modulate cell adhesion and migration (Zou et al., 2004), consistent with the misalignment of both growth plate chondrocytes and the axis of joint formation in *Jaws*$^{-/-}$ embryos. Moreover, the particular importance of CS sulfation for chondrogenesis may explain why mutation of *Jaws*, a widely expressed gene, produces defects that are relatively specific to endochondral ossification.

Importantly, this genetic loss-of-function approach distinguishes our findings from previous demonstrations of ectopic joint formation caused by overexpressing Wnt9a or activated β-catenin in vivo or by blocking α5β1 integrin function in limb explant cultures (Hartmann

DEVELOPMENT

and Tabin, 2001; Guo et al., 2004; Garciadiego-Cázares et al., 2004). Our findings also contrast with data obtained by inactivation of the hypoxia-inducible factor 1 α (*Hif1a*) gene in mouse limb mesenchyme. Conditional deletion of *Hif1a* using *Prx1-Cre* produces longitudinal cavities that are superficially similar to those seen in *Jaws*$^{-/-}$ digits; however, unlike ectopic *Jaws*$^{-/-}$ joints, *Hif1a*-null cavities form prior to the wild-type joint interzone and do not express joint markers such as *Wnt9a* and *Bmp2* (Amarilio et al., 2007; Provot et al., 2007). *Gdf5* is expressed primarily in diffuse transverse (rather than longitudinal) stripes in *Hif1a*-null digits, leading Provot and colleagues to conclude that after an initial developmental delay, synovial joints of normal appearance do form in the digits of these mice. Together, data presented by both groups argue that the *Hif1a*-null digit phenotype reflects delayed joint specification caused by aberrant differentiation of hypoxic chondrocytes.

By demonstrating the persistence of ectopic joints in *Jaws*$^{-/-}$ digits, our studies identify JAWS as a novel regulator in the establishment of the interphalangeal joint axes. Because cells in the ectopic *Jaws*$^{-/-}$ joint express appropriate early interzone markers (Fig. 3B,C), we conclude that the molecular specification and the spatial positioning of the synovial joint interzone are genetically separable processes. Similarly, the restriction of ectopic joints to digits and the lack of knee joints in *Jaws*$^{-/-}$ embryos support the notion that distinct *Jaws*-dependent mechanisms govern synovial joint development at different sites in the embryonic skeleton. Overall, *Jaws*$^{-/-}$ mice provide a unique animal model for exploring the tightly coordinated processes of chondrogenesis and joint morphogenesis, and for better understanding the etiology of joint degeneration leading to debilitating diseases such as osteoarthritis.

Supplementary material

Supplementary material for this article is available at http://dev.biologists.org/cgi/content/full/135/13/2215/DC1

References

Akiyama, H., Chaboissier, M. C., Martin, J. F., Schedl, A. and de Crombrugghe, B. (2002). The transcription factor Sox9 has essential roles in successive steps of the chondrocyte differentiation pathway and is required for expression of Sox5 and Sox6. *Genes Dev.* **16**, 2813-2828.

Amarilio, R., Viukov, S. V., Sharir, A., Eshkar-Oren, I., Johnson, R. S. and Zelzer, E. (2007). HIF1α regulation of Sox9 is necessary to maintain differentiation of hypoxic prechondrogenic cells during early skeletogenesis. *Development* **134**, 3917-3928.

Arner, E. C. (2002). Aggrecanase-mediated cartilage degradation. *Curr. Opin. Pharmacol.* **2**, 322-329.

Baur, S. T., Mai, J. J. and Dymecki, S. M. (2000). Combinatorial signaling through BMP receptor IB and GDF5: shaping of the distal mouse limb and the genetics of distal limb diversity. *Development* **127**, 605-619.

Gao, G., Plaas, A., Thompson, V. P., Jin, S., Zuo, F. and Sandy, J. D. (2004). ADAMTS4 (aggrecanase-1) activation on the cell surface involves C-terminal cleavage by glycosylphosphatidyl inositol-anchored membrane type 4-matrix metalloproteinase and binding of the activated proteinase to chondroitin sulfate and heparan sulfate on syndecan-1. *J. Biol. Chem.* **279**, 10042-10051.

Garciadiego-Cazares, D., Rosales, C., Katoh, M. and Chimal-Monroy, J. (2004). Coordination of chondrocyte differentiation and joint formation by α5β1 integrin in the developing appendicular skeleton. *Development* **131**, 4735-4742.

Glass, D. A., 2nd, Bialek, P., Ahn, J. D., Starbuck, M., Patel, M. S., Clevers, H., Taketo, M. M., Long, F., McMahon, A. P., Lang, R. A. et al. (2005). Canonical Wnt signaling in differentiated osteoblasts controls osteoclast differentiation. *Dev. Cell* **8**, 751-764.

Guo, X., Day, T. F., Jiang, X., Garrett-Beal, L., Topol, L. and Yang, Y. (2004). Wnt/β-catenin signaling is sufficient and necessary for synovial joint formation. *Genes Dev.* **18**, 2404-2417.

Hartmann, C. and Tabin, C. J. (2001). Wnt-14 plays a pivotal role in inducing synovial joint formation in the developing appendicular skeleton. *Cell* **104**, 341-351.

Hill, T. P., Spater, D., Taketo, M. M., Birchmeier, W. and Hartmann, C. (2005). Canonical Wnt/beta-catenin signaling prevents osteoblasts from differentiating into chondrocytes. *Dev. Cell* **8**, 727-738.

Khan, I. M., Redman, S. N., Williams, R., Dowthwaite, G. P., Oldfield, S. F. and Archer, C. W. (2007). The development of synovial joints. *Curr. Top. Dev. Biol.* **79**, 1-36.

Kiani, C., Lee, V., Cao, L., Chen, L., Wu, Y., Zhang, Y., Adams, M. E. and Yang, B. B. (2001). Roles of aggrecan domains in biosynthesis, modification of glycosaminoglycans and product secretion. *Biochem. J.* **354**, 199-207.

Klüppel, M., Wight, T. N., Chan, C., Hinek, A. and Wrana, J. L. (2005). Maintenance of chondroitin sulfation balance by chondroitin-4-sulfotransferase 1 is required for chondrocyte development and growth factor signaling during cartilage morphogenesis. *Development* **132**, 3989-4003.

Koziel, L., Kunath, M., Kelly, O. G. and Vortkamp, A. (2004). Ext1-dependent heparan sulfate regulates the range of Ihh signaling during endochondral ossification. *Dev. Cell* **6**, 801-813.

Kronenberg, H. M. (2003). Developmental regulation of the growth plate. *Nature* **423**, 332-336.

Mak, K. K., Chen, M. H., Day, T. F., Chuang, P. T. and Yang, Y. (2006). Wnt/beta-catenin signaling interacts differentially with Ihh signaling in controlling endochondral bone and synovial joint formation. *Development* **133**, 3695-3707.

Mitchell, K. J., Pinson, K. I., Kelly, O. G., Brennan, J., Zupicich, J., Scherz, P., Leighton, P. A., Goodrich, L. V., Lu, X., Avery, B. J. et al. (2001). Functional analysis of secreted and transmembrane proteins critical to mouse development. *Nat. Genet.* **28**, 241-249.

Mitrovic, D. R. (1977). Development of the metatarsophalangeal joint of the chick embryo: morphological, ultrastructural and histochemical studies. *Am. J. Anat.* **150**, 333-347.

Nagy, A. (2003). *Manipulating the Mouse Embryo: A Laboratory Manual*. Cold Spring Harbor, NY: Cold Spring Harbor Laboratory Press.

Pacifici, M., Koyama, E. and Iwamoto, M. (2005). Mechanisms of synovial joint and articular cartilage formation: recent advances, but many lingering mysteries. *Birth Defects Res. C Embryo Today* **75**, 237-248.

Pitsillides, A. A. (1999). The role of hyaluronan in joint cavitation. In *Biology of the Synovial Joint* (ed. C. W. Archer, B. Caterson, M. Benjamin and J. R. Ralphs), pp. 41-62. London: Informa Healthcare.

Plaas, A. H., West, L., Midura, R. J. and Hascall, V. C. (2001). Disaccharide composition of hyaluronan and chondroitin/dermatan sulfate. Analysis with fluorophore-assisted carbohydrate electrophoresis. *Methods Mol. Biol.* **171**, 117-128.

Provot, S., Zinyk, D., Gunes, Y., Kathri, R., Le, Q., Kronenberg, H. M., Johnson, R. S., Longaker, M. T., Giaccia, A. J. and Schipani, E. (2007). Hif-1α regulates differentiation of limb bud mesenchyme and joint development. *J. Cell Biol.* **177**, 451-464.

Schwartz, N. B. and Domowicz, M. (2002). Chondrodysplasias due to proteoglycan defects. *Glycobiology* **12**, 57R-68R.

Schweitzer, R., Chyung, J. H., Murtaugh, L. C., Brent, A. E., Rosen, V., Olson, E. N., Lassar, A. and Tabin, C. J. (2001). Analysis of the tendon cell fate using Scleraxis, a specific marker for tendons and ligaments. *Development* **128**, 3855-3866.

Skarnes, W. C., Moss, J. E., Hurtley, S. M. and Beddington, R. S. (1995). Capturing genes encoding membrane and secreted proteins important for mouse development. *Proc. Natl. Acad. Sci. USA* **92**, 6592-6596.

St-Jacques, B., Hammerschmidt, M. and McMahon, A. P. (1999). Indian hedgehog signaling regulates proliferation and differentiation of chondrocytes and is essential for bone formation. *Genes Dev.* **13**, 2072-2086.

Tortorella, M., Pratta, M., Liu, R. Q., Abbaszade, I., Ross, H., Burn, T. and Arner, E. (2000). The thrombospondin motif of aggrecanase-1 (ADAMTS-4) is critical for aggrecan substrate recognition and cleavage. *J. Biol. Chem.* **275**, 25791-25797.

Yi, S. E., Daluiski, A., Pederson, R., Rosen, V. and Lyons, K. M. (2000). The type I BMP receptor BMPRIB is required for chondrogenesis in the mouse limb. *Development* **127**, 621-630.

Zhao, W., Sala-Newby, G. B. and Dhoot, G. K. (2006). Sulf1 expression pattern and its role in cartilage and joint development. *Dev. Dyn.* **235**, 3327-3335.

Zou, X. H., Foong, W. C., Cao, T., Bay, B. H., Ouyang, H. W. and Yip, G. W. (2004). Chondroitin sulfate in palatal wound healing. *J. Dent. Res.* **83**, 880-885.